Journal of Metals, Materials and Minerals, 34(3), 2055, 2024

Synthesis and visible light photocatalytic activity of silver zinc phosphates

Rina KANEMOTO[1], and Hiroaki ONODA[2,*]

[1] *Department of Informatics and Environmental Sciences, Faculty of Life and Environmental Sciences, Kyoto Prefectural University, 1-5, Shimogamo Nakaragi-cyo, Sakyo-ku, Kyoto 606-8522, Japan*

[2] *Department of Biomolecular Chemistry, Faculty of Science and Technology, Kyoto Prefectural University, 1-5, Shimogamo Nakaragi-cyo, Sakyo-ku, Kyoto 606-8522, Japan*

***Corresponding author e-mail**: h-onoda@kpu.ac.jp

Received date:
14 May 2024
Revised date:
22 August 2024
Accepted date:
23 August 2024

Keywords:
Silver phosphate;
Visible light photocatalytic activity;
Antimicrobial activity

Abstract

Currently, photocatalytic materials in common use mainly use ultraviolet light, but the amount of ultraviolet light contained in sunlight is limited and their energy efficiency is known to be low. Therefore, there is a need for a compound that shows photocatalytic activity in visible light, and silver phosphate matches this requirement, but it is relatively expensive. In this study, photocatalytic materials that could use visible light and were relatively inexpensive were attempted to be prepared. Specifically, samples were prepared by changing the silver/zinc molar ratio (Ag/Zn = 100/0, 90/10, 80/20, 70/30, 60/40), and each sample was evaluated and examined from chemical composition, particle size, and functionality (UV-Vis. reflectance spectra, photocatalytic activity evaluation using methylene blue degradation reaction, and antibacterial property evaluation). It was found that silver phosphate was formed even in the sample with the lowest silver ratio, Ag/Zn = 60/40, showing high visible light responsive photocatalytic activity and antibacterial activity against *E. coli*.

1. Introduction

A catalyst is a substance that affects the rate of a chemical reaction without itself changing, and generally refers to a substance that speeds up a chemical reaction [1]. Among them, catalysts that work with light as an energy source are called photocatalysts [2,3]. The specific process involves the decomposition of water molecules and oxygen in the air by pairs of electrons (e-) and holes (h+) generated when the material absorbs light energy, which are converted into radical species with strong oxidative power, breaking down organic matter and killing bacteria [4,5]. The addition of materials with these functional properties to paints and other materials provides antibacterial, anti-odor and stain-resistant effects [6-9]. However, at present, commonly used photocatalytic materials are mainly UV-based materials such as titanium dioxide and zinc oxide, which can only be applied outdoors and have poor energy efficiency, as the amount of UV radiation in sunlight is limited to about 7% [10]. There is therefore a need to develop photocatalytic materials acting on visible light that can be used indoors. Visible light is about 56% of sunlight, as well as fluorescent lamps and LEDs, and is therefore expected to improve energy efficiency and have applications both indoors and outdoors [11,12]. Until now, new materials exhibiting excellent photocatalytic properties have been investigated by combining simple metal oxides with p-blocking elements, alkali metal elements or alkaline earth metal elements [13-16]. Among them, bismuth vanadate, tungsten oxide and silver phosphate are mentioned as materials that show photocatalytic activity in visible light and can be applied both indoors and outdoors. In particular, silver phosphate has been reported to have a better ability to carry out photooxidative degradation of water under visible light than other visible light photocatalytic materials such as bismuth vanadate and tungsten oxide, and is expected to be applied to artificial photosynthesis [17-19]. It is a yellow powder with a body-centered cubic structure [20]. In addition, silver compounds are expected to have antibacterial properties due to silver ions [21]. On the other hand, silver phosphate is relatively expensive because it uses silver, and its practical application is difficult [22,23]. Therefore, there is a need to develop less expensive materials. Therefore, in this study, silver phosphate, a visible light-responsive photocatalyst, was used to reduce the cost by replacing some of the silver cations with zinc cations, and to improve the photocatalytic activity with visible light.

Hydrothermal synthesis is a sample preparation method that allows the synthesis of compounds and crystal growth with relatively small energy consumption in the presence of hot water at high temperature and pressure [24-26]. The pH of the solvent is also an important factor in the preparation of silver phosphate. It has also been reported that the shape, particle size and photocatalytic activity of silver phosphate vary depending on the phosphate source used [27]. It is known that when metal ions become supersaturated, insoluble compounds are formed in aqueous solution, which is dependent on pH, with particles forming more easily at higher pH value. When supersaturated conditions are maintained, these insoluble substances are known to aggregate and form the nuclei of ultrafine particles. Therefore, the morphology and particle size of silver phosphate can be affected by changing the pH value during sample preparation, which may improve its photocatalytic activity. Therefore, this study also investigated the effect of the pH value of the solvent on the products.

2. Experimental

Figure 1 shows the preparation procedure of samples. Silver nitrate was added to a solution of 2 mL of phosphoric acid (2.8 mol·L^{-1}) diluted with 10 mL of water at a ratio of Ag/P = 3/1 and allowed to stand for 1 day. The mixture was placed in an autoclave (98 mL) and heated at 160°C for 20 h. Acetone (50 mL) was then added to the mixture to form a precipitate and facilitate the removal of excess water. The precipitate was then filtered and dried. Part of the silver nitrate was replaced by zinc nitrate in the ratio Ag:Zn:P=x:(100-x):(200-x)/3, (x=90, 80, 70, 60), and hydrothermal treatment was carried out in a similar way. This mixing ratio was determined by the fact that silver ions are monovalent, zinc ions are divalent, and phosphate ions are trivalent. In addition, samples with Ag/Zn = 60/40 were prepared at pH 4, 7 and 10 with 8 mol·L^{-1} of sodium hydroxide solution prior to hydrothermal synthesis (initial pH: 1-2). All chemicals were of commercial purity (FUJIFILM Wako Pure Chemical Corp., Osaka, Japan) and used without further purification.

The crystal structure and chemical bonding of these materials were analyzed using X-ray diffraction (XRD) patterns and infrared (IR) spectra, respectively. XRD patterns were recorded on an X-ray diffractometer (MiniFlex, Rigaku Corp., Akishima, Japan) using monochromatic CuKα radiation (30 kV, 15 mA, 3°·min^{-1}, step size: 0.02°). The IR spectra of the samples were recorded by the KBr disk method (Resolution: 4 cm^{-1}, 16 times scanned) using a HORIBA Fourier-transform infrared (FT-IR) 720 (HORIBA Corp., Kyoto, Japan).

Scanning Electron Microscope (SEM) images of the samples were recorded using a MiniscopeR TM3030Plus (Hitachi High-Tech Corp., Tokyo, Japan) with an accelerating voltage of 5kV/15kV. The color of phosphate powders was estimated from the ultraviolet-visible (UV-Vis) reflectance spectrum (UV2100; Shimadzu Corporation, Kyoto, Japan) (reference compound: $BaSO_4$).

The photocatalytic activity of samples was estimated with the decomposition of methylene blue by LED light. The 0.01 g of sample was placed in 4 mL of methylene blue solution (1.0×10^{-5} mol·L^{-1}), and then this solution was radiated. The decrease of the absorption at about 660 nm was estimated for 120 min. To ensure that the evaluation of photocatalytic activity was not disturbed by the adsorption of the sample itself, the photocatalytic activity was evaluated one day after the sample was added to the methylene blue solution. Furthermore, the photocatalytic activity was also tested three times for re-use and found to be unchanged.

Antibacterial activity was evaluated using *Escherichia coli* (Dh5α). Samples were dry heat sterilized (200°C, 3 h), dissolved in sterile distilled water, and stored in the dark except when used. *E. coli* (Dh5α) was inoculated from colonies into 5 mL of LB broth, shaken and cultured overnight and measured spectrophotometrically, using log phase *E. coli* with OD600 = 0.9 Abs. Then 1.5 mL of *E. coli* was centrifuged (7000 rpm × 5 min, 4°C), the supernatant was discarded, sterile saline was added, and then centrifuged. The same procedure was repeated twice. The 10 μL of diluted *E. coli* solution was mixed with 20 mL of sterile saline and 20 μL of sample solution and shaken overnight. Each petri dish was then inoculated with 10 μL and incubated at 37°C overnight. The antimicrobial activity was evaluated by CFU (colony forming units)/mL on the following day and examining the survival rate of *E. coli* relative to CFU for overnight treatment without the sample solution.

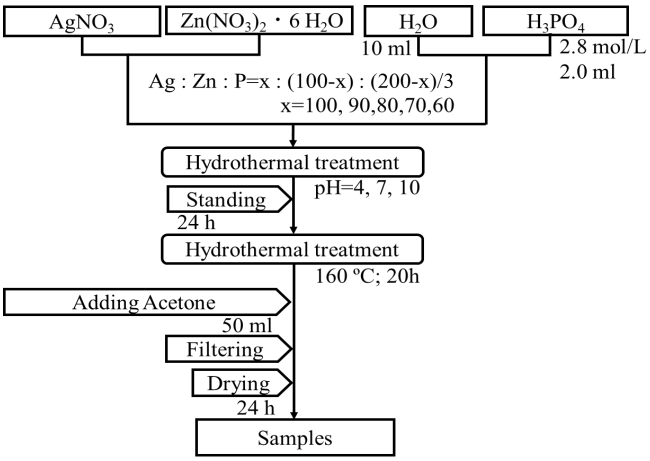

Figure 1. Preparation method of samples.

3. Results and discussion

Figure 2 shows the XRD patterns of samples prepared in various Ag/Zn ratios. The XRD patterns of all samples had Ag_3PO_4 peaks, indicating that the main composition of the samples was this compound [28]. The peak intensity did not change as the ratio of silver ions decreased. On the other hand, there are no peaks of zinc phosphate, zinc oxide, silver nitrate, or zinc nitrate were observed. It was considered that silver phosphate precipitates more easily than zinc phosphate, and that the first crystallization of silver phosphate inhibits the crystallization of zinc phosphate, so that the zinc phosphate peak is not observed.

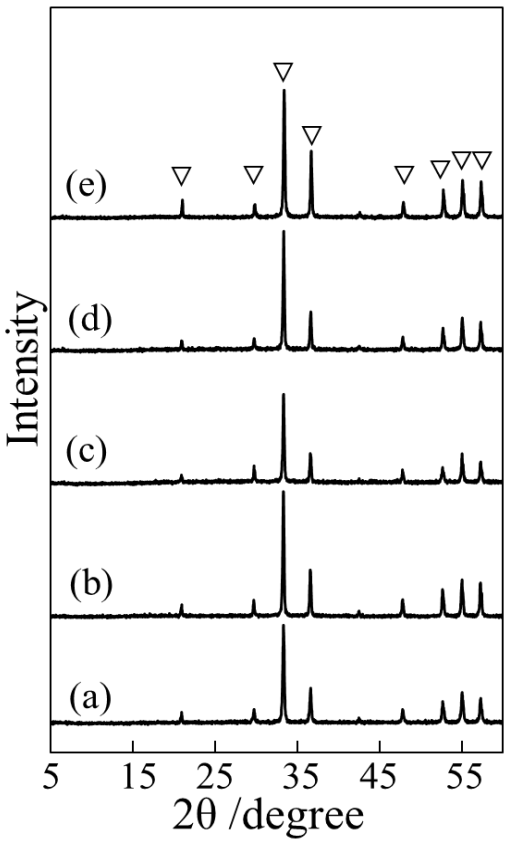

Figure 2. XRD patterns of samples prepared in various Ag/Zn ratios, (a) Ag/Zn =100/0, (b) 90/10, (c) 80/20, (d) 70/30, (e) 60/40, ▽; Ag_3PO_4.

Figure 3 shows the IR spectra of samples prepared in various Ag/Zn ratios. The asymmetric stretching vibration peak of the P-O bond near 1050 cm^{-1} and the phosphate bond peak due to O-P-O declination vibration near 540 cm^{-1} indicated that the prepared sample contained phosphate. The O-H bond angular vibration peak near 1650 cm^{-1} was attributed to water in the sample. In XRD patterns and IR spectra, little change was observed with Ag/Zn ratio. It was considered that silver phosphates crystallise and precipitate more easily than zinc salts, resulting in a higher proportion of silver than the prepared ratio and therefore unlikely to show ratio-dependent changes.

Samples were dissolved in acid solution and the Ag/Zn ratio in the samples was determined. However, it was difficult to calculate reliable values due to differences in the solubility of the Ag and Zn compounds. It was considered certain that the samples contained a higher proportion of silver than the composition of the preparation.

Figure 4 shows the UV-Vis. reflectance spectra of samples prepared in various Ag/Zn ratios. All samples have absorption around 400 nm to 500 nm in the visible light region, indicating that the samples are yellow powders. The light absorbed in this region is used as an energy source for photocatalytic activity. Furthermore, due to the narrow absorption wavelength range, it is believed that photocatalytic reactions can be triggered by irradiation of light at specific wavelengths. The reflectance increased as the silver ratio decreased, which was attributed to the white color of the zinc compound.

Figure 5 shows the SEM images of samples prepared in various Ag/Zn ratios. Fine columnar particles were observed in all samples. Samples prepared in Ag/Zn = 100/0 and 90/10 had particles with the sizes of 10 μm to 20 μm, indicating that the hydrothermal synthesis method promotes particle growth. On the other hand, samples prepared in Ag/Zn = 80/20, 70/30, and 60/40 have particles of 5 μm to 10 μm mixed with smaller particles, indicating that the particles have not grown sufficiently. In Figure 5(e), the shiny layer seen in Figure 5(c,d) was no longer present due to the smaller particles. The high ratio of zinc ions was thought to inhibit the growth of silver phosphate particles. Regarding the shape of the particles, it was found that silver phosphate alone forms columnar particles. Furthermore, it was also shown that the zinc-substituted samples also exhibited a similar particle shape.

Figure 6 shows the EDX mapping image of sample prepared in Ag/Zn = 60/40. It is shown that Ag, O, and P are almost uniformly distributed on the particle surface of the sample. This result indicates that silver phosphate is uniformly present on the particle surface of the sample, even if the silver ratio is low. On the other hand, zinc ions were not found on the sample surface. This phenomenon was thought to be caused by the solubility of the zinc compounds being higher than that of the silver compounds.

Figure 7 shows the residual ratio of absorbance with methylene blue when samples prepared with various Ag/Zn ratios are used as photocatalysts. A high reduction ratio means the strong photocatalytic activity. The photocatalytic activity of all samples decreased in absorbance over time, qualitatively indicating photocatalytic activity under visible light. Furthermore, sample prepared in Ag/Zn = 60/40 showed a remarkable reduction ratio, which can be attributed to the fine particle size (Figure 5) and the uniform distribution of silver phosphate on the particle surface (Figure 6) [29].

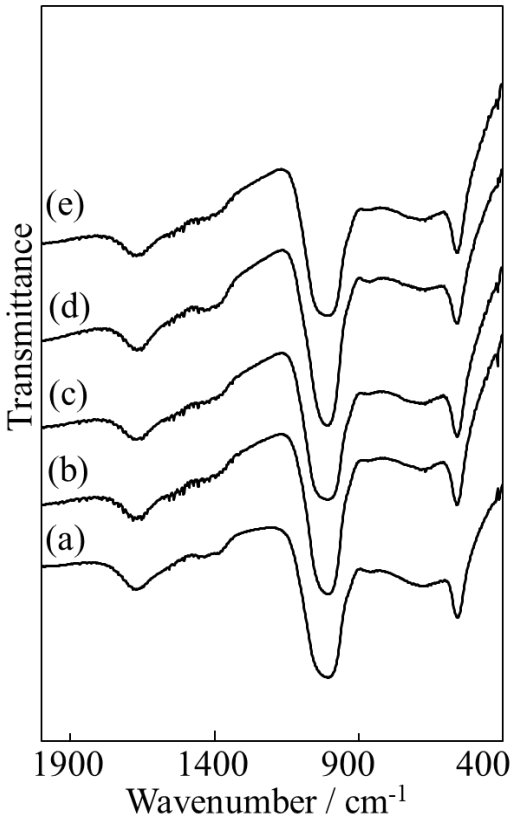

Figure 3. IR spectra of samples prepared in various Ag/Zn ratios, (a) 100/0, (b) 90/10, (c) 80/20, (d) 70/30, (e) 60/40.

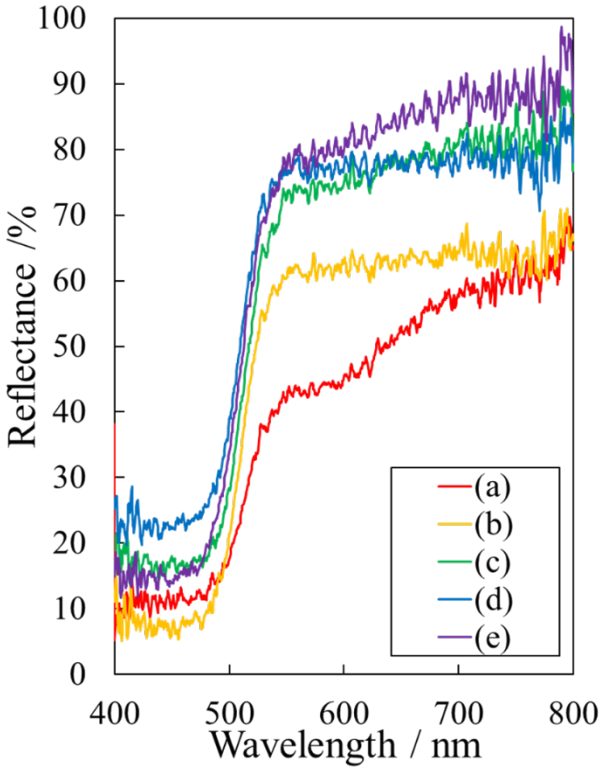

Figure 4. UV-Vis. reflectance spectra of samples prepared in various Ag/Zn ratios, (a) 100/0, (b) 90/10, (c) 80/20, (d) 70/30, (e) 60/40.

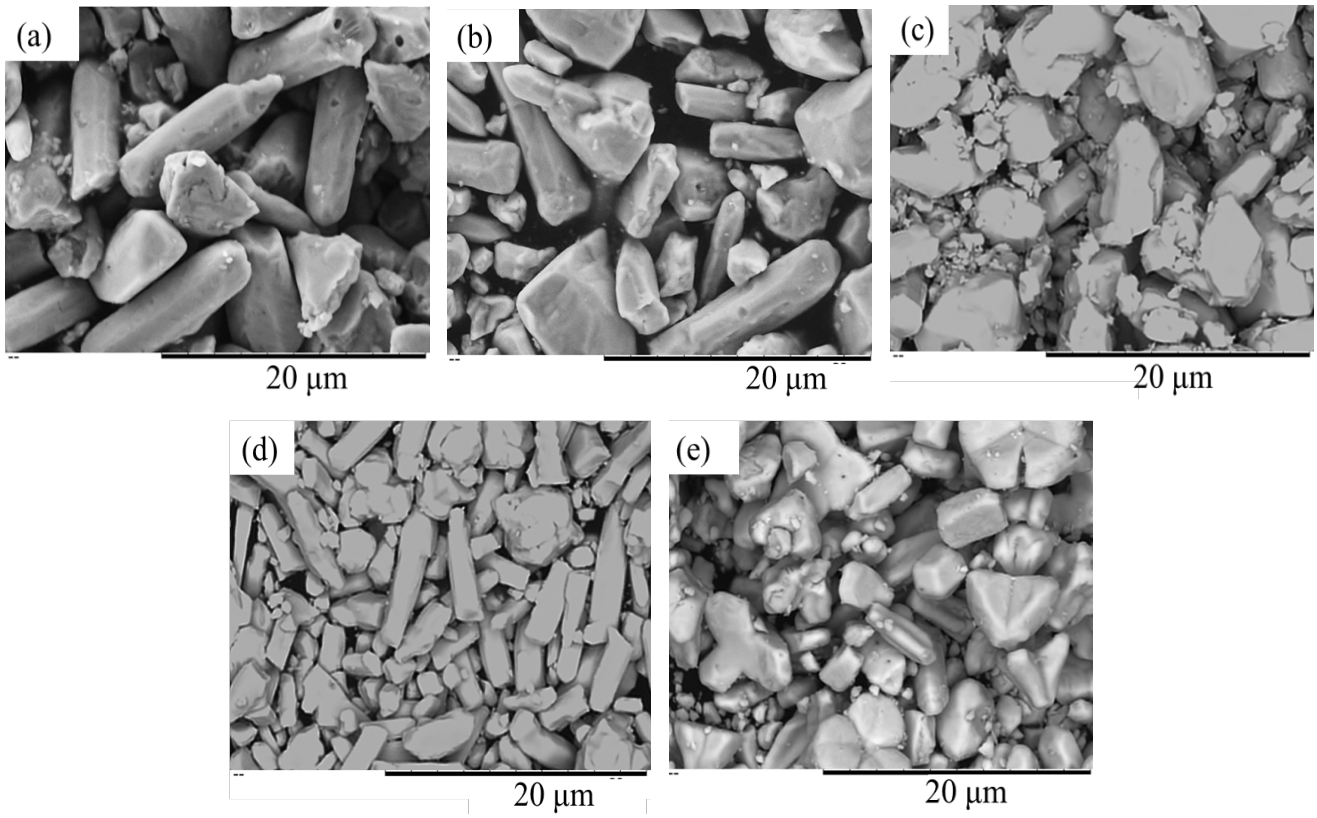

Figure 5. SEM images of samples prepared in various Ag/Zn ratios, (a) 100/0, (b) 90/10, (c) 80/20, (d) 70/30, (e) 60/40.

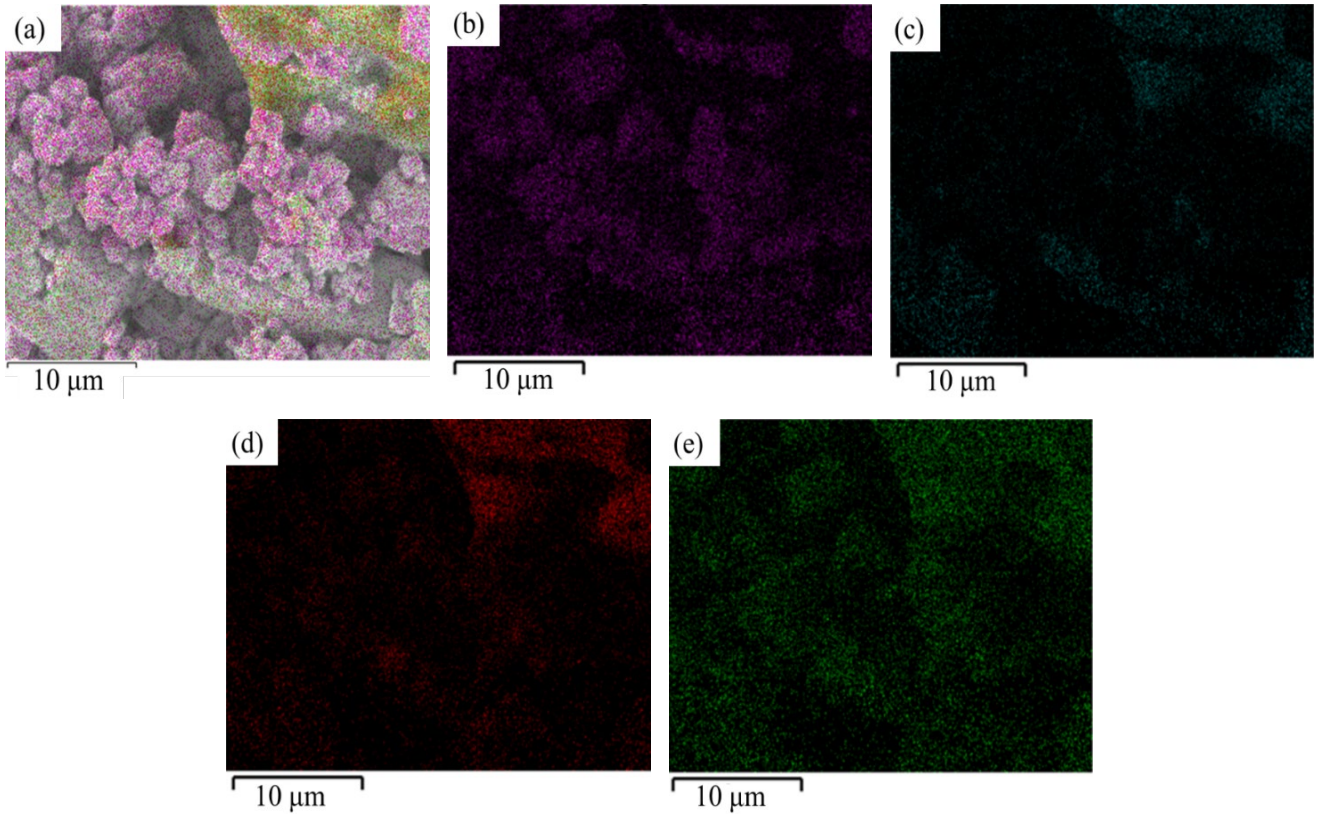

Figure 6. EDX images of the sample prepared in Ag/Zn=60/40 at pH = 4, (a) layer images, (b) Ag, (c) Zn, (d) O, (e) P.

Table 1 shows the antibacterial activity of samples prepared in various Ag/Zn ratios. In the control with no sample added, *E. coli* increased with time. Under conditions with phosphate samples, *E. coli* increased up to 60 min after incubation. However, after 120 min, all samples had low *E.coli* concentrations. This indicates that the samples showed antimicrobial activity when in contact with *E. coli* for more than 60 min. Sample prepared with Ag/Zn = 80/20 had a higher number of colonies after 120 min than sample without zinc substitution. Furthermore, samples with a higher ratio of zinc were more affected by particle size than by zinc substitution, with a decrease in the number of colonies after 120 min. In particular, the sample with Ag/Zn=60/40 showed the highest antimicrobial activity. This may be due to an increase in the surface area in contact with *E. coli* and surface silver phosphate due to the finer particle size, as described in Figure 5.

Figure 8 shows the SEM images of samples prepared in Ag/Zn = 60/40 at various pH values. Sample prepared at pH 4 contained a mixture of large columnar particles of approximately 20 μm and cubic or spherical fine particles. In the sample prepared at pH 7, the particle size was relatively uniform around 7.5 μm, and the particle shape was mostly spherical with a few thin columnar particles. The particle size of the sample prepared at pH 10 was relatively uniform at about 2 μm. The particle shape showed spherical and irregular fine particles. As a result, the particle size was smaller than that of samples prepared without pH adjustment shown in Figure 5. The effect of this on photocatalytic activity was investigated, and the results are shown in Figure 9, indicating that the higher the pH value, the greater the reduction ratio of absorbance with methylene blue, this means the higher the photocatalytic activity. This may be attributable to the decrease in particle size with increasing pH value, resulting in an increase in surface area (Figure 8). Furthermore, for sample prepared at pH 10, the particle shape increased the surface area, suggesting a significant increase in photocatalytic activity. Due to slightly different experimental conditions, the residual ratios in Figure 9 are higher than those in Figure 7, and therefore no comparison can be made between the two.

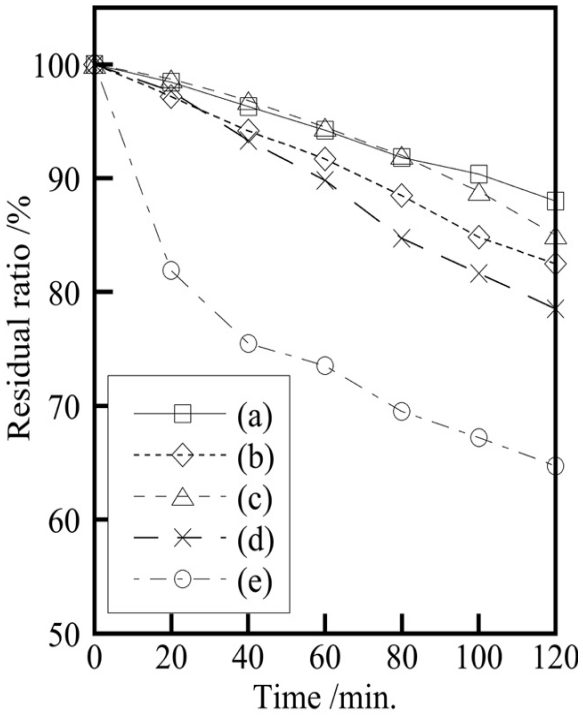

Figure 7. Residual ratio of absorbance with methylene blue due to photocatalytic activity of samples prepared in various Ag/Zn ratios, (a) 100/0, (b) 90/10, (c) 80/20, (d) 70/30, (e) 60/40.

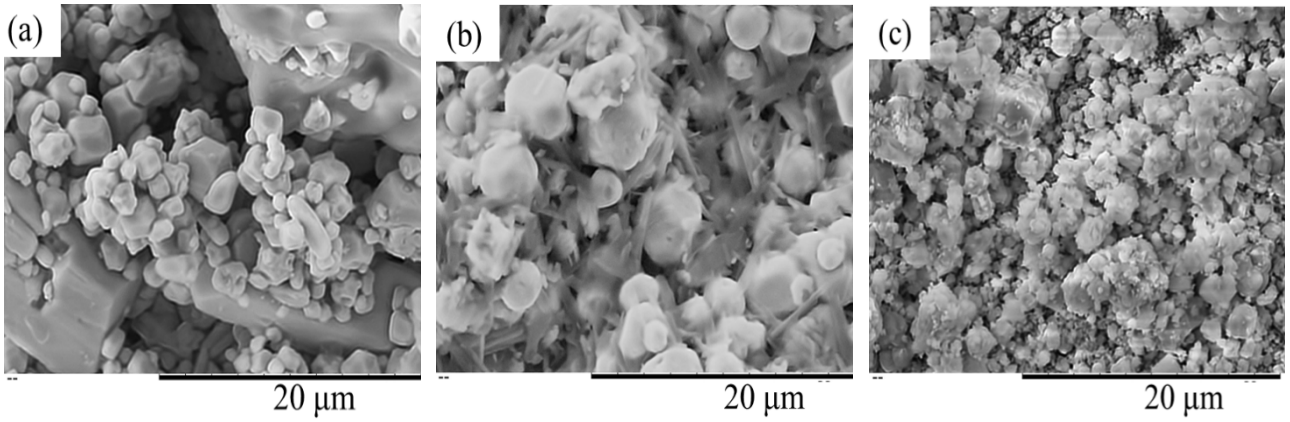

Figure 8. SEM images of samples prepared in Ag/Zn=60/40 at various pH, (a) 4, (b) 7, (c) 10.

Table 1. Visible E.coli concentration (×10⁴ CFU/ml) with samples prepared in various Ag/Zn ratios

Time (min)	0	60	120
Control	2.3	19.5	24.7
Ag/Zn=100/0	2.3	10.7	3.7
Ag/Zn=80/20	2.3	12.2	8.8
Ag/Zn=70/30	2.3	15.4	6.4
Ag/Zn=60/40	2.3	10.8	2.6

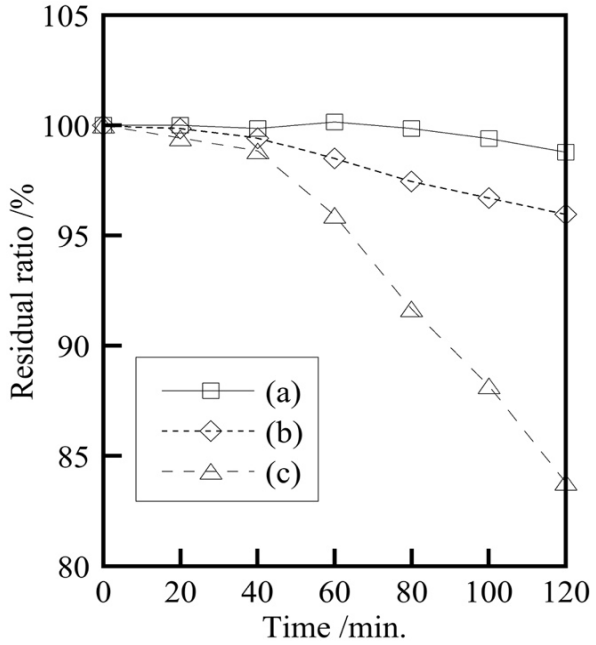

Figure 9. Residual ratio of absorbance with methylene blue due to photocatalytic activity of samples prepared in Ag/Zn=60/40 at various pH, (a) 4, (b) 7, (c) 10.

4. Conclusions

The phosphate visible-light responsive photocatalysts were prepared by hydrothermal synthesis in various Ag/Zn ratios. SEM images show that the silver phosphate particles were columnar, and that the particles became smaller as the zinc ratio increased. The photocatalytic activity of the phosphates was enhanced by zinc substitution. This provides a positive prospect for the development of low-cost materials with improved photocatalytic performance by preparing materials with zinc substitution rather than silver phosphate alone. Furthermore, samples in this study showed effective antimicrobial activity against *E. coli*, especially those prepared with Ag/Zn = 60/40, even at lower silver concentrations. In addition, samples prepared at higher pH showed higher photocatalytic activity, indicating that pH has a significant effect on particle size and particle shape, contributing to higher photocatalytic activity.

Conflict of interest

The authors declare that they have no conflict of interest.

Acknowledgment

The authors are grateful to Mr. Kikuya Ogata, Kyoto Municipal Institute of Industrial Technology and Culture, Japan, for SEM-EDX measurements.

References

[1] G. Job, and F. Herrmann, "Chemical potential—a quantity in search of recognition. *European Journal of Physics*, vol. 27, no. 2, p. 353, 2006.

[2] H. Ahmad, S. K. Kamarudin, L. J. Minggu, and M. Kassim, "Hydrogen from photo-catalytic water splitting process: A review," *Renewable and Sustainable Energy Reviews,* vol. 43, pp. 599-610, 2015.

[3] S. Zhu, and D. Wang, "Photocatalysis: Basic principles, diverse forms of implementations and emerging scientific opportunities," *Advanced Energy* Materials, vol. 7, p. 1700841, 2017.

[4] J. Z. Hassan, A. Raza, U. Qumar, and G. Li, "Recent advances in engineering strategies of Bi-based photocatalysts for environmental remediation," *Sustainable Materials and Technologies,* vol. 33, p. e00478, 2022.

[5] A. Nairan, Z. Feng, R. Zheng, U. Khan, and J. Ga, "Engineering metallic alloy electrode for robust and active water electrocatalysis with large current density exceeding 2000 $mA \cdot cm^{-2}$," vol. 36, no. 29, p. 2401448, 2024.

[6] S. A. Ruffolo, M. F. La Russa, M. Malagodi, C. Oliviero, A. M. Palermo, and G. M. Crici, "ZnO and $ZnTiO_3$ nanopowders for antimicrobial stone coating," *Applied Physics A.,* vol. 100, no. 3, pp. 829-834, 2010.

[7] W. Promsuwan, P. Sujaridworakun, and W. Reainthippayasakul, "Synthesis of zinc oxide photocatalysts from zinc-dust waste for organic dye degradation," *Journal of Metals, Materials and Minerals*, vol. 33, no. 2, pp. 58-64, 2023.

[8] S. Li, K. Dong, M. Cai, X. Li, and X. Chen, "A plasmonic S-scheme Au/MIL 101(Fe)/BiOBr photocatalyst for efficient synchronous decontamination of Cr(VI) and norfloxacin antibiotic," *eScience*, vol. 4, no. 2, p. 100208, 2024.

[9] C. Wang, K. Rong, Y. Liu, F. Yang, and S. Li, "Carbon quantum dots-modified tetra (4-carboxyphenyl) porphyrin/ BiOBr S-scheme heterojunction for efficient photocatalytic antibiotic degradation," *Science China Materials*, vol. 67, no. 2, pp. 562-572, 2024.

[10] Q. Li, Y. W. Li, P. Wu, R. Xie, and J. K.Shang, "Palladium oxide nanoparticles on nitrogen-doped titanium oxide: accelerated photocatalytic disinfection and post-illumination catalytic "memory"," *Advanced Materials,* vol. 20, no. 19, pp. 3717-3723, 2008.

[11] S. Rajagopal, R. D. Roberts, and S. K. Lim, "Visible light communication: Modulation schemes and dimming support," *IEEE Communications Magazine*, vol. 50, no. 3, pp. 72-82, 2012.

[12] S. Dong, J. Feng, M. Fan, Y. Pi, L. Hu, M. Liu, J. Sun, and C. Du, "Recent developments in heterogeneous photocatalytic water treatment using visible light-responsive photocatalysts: A review," *RSC Advances,* vol. 5, no. 19, p. 14610, 2015.

[13] H. Tong, S. Ouyang, Y. Bi, N. Umezawa, M. Oshikiri, and J. Ye, "Nano-photocatalytic materials: Possibilities and challenges," *Advanced Materials*, vol. 24, no. 2, pp. 229-251, 2012.

[14] M. V. Dozzi, and E. Selli, , "Doping TiO_2 with p-block elements: Effects on photocatalytic activity," *Journal of Photochemistry and Photobiology C: Photochemistry Reviews*, vol. 14, pp. 13-28, 2013.

[15] C. Tangwongputti, P. Reubroycharoen, and P. Sujaridworakun, "Facile synthesis of heterostructured g-C_3N_4/Ag-TiO_2 photocatalysts with enhanced visible-light photocatalytic performance," *Journal of Metals, Materials and Minerals*, vol. 32, no. 1, pp. 48-54, 2022.

[16] S. Li, C. You, K. Rong, C. Zhuang, X. Chen, and B. Zhang, "Chemically bonded $Mn_{0.5}Cd_{0.5}S$/BiOBr S-scheme photocatalyst with rich oxygen vacancies for improved photocatalytic decontamination performance," *Advanced Powder Materials,* vol. 3, p. 100183, 2024.

[17] E. S. Kim, H. Kang, G. Magesh, J. Y. Kin, J-W Jang, and J. S. Lee, "Improved photoelectrochemical activity of $CaFe_2O_4$/$BiVO_4$ heterojunction photoanode by reduced surface recombination in solar water oxidation," *ACS Applied Materials and Interfaces*, vol. 6, p. 17762, 2014.

[18] Q. Zheng, D. P. Durkin, J. E. Elenewski, Y. Sun, N. A. Banek, L Hua, H. Chen, M. J. Wagner, W. Zhang, and D. Shuai, "Visible-light-responsive graphitic carbon nitride: rational design and photocatalytic applications for water treatment," *Environmental Science & Technology,* vol. 50, no. 23, p. 12938, 2016.

[19] M. G. Lee, J. S. Park, and H. W. Jang, "Solution-processed metal oxide thin film nanostructures for water splitting photo-electrodes: A review," *Journal of the Korean Ceramic Society*, vol. 55, no. 3, pp. 185-202, 2018.

[20] A. Amirulsyafiee, M. M. Khan, and M. Y. Khan, "Visible light active La-doped Ag_3PO_4 for photocatalytic degradation of dyes and reduction of Cr (VI)," *Solid State Sciences*, vol. 131, p. 106950, 2022.

[21] Y. J. Cheng, D. N. Zeiger, J. A. Howarter, X. Zhang, N.J. Lin, J. M. Antonucci, and S. Lin-Gibson, "In situ formation of silver nanoparticles in photocrosslinking polymers," *Journal of Biomedical Materials Research Part B Applied Biomaterials*, vol. 97, no. 1, pp. 124-131, 2011.

[22] S. Guo, Y. Jiang, F. Wu, P. Yu, H. Liu, Y. Li, and L Mao, "Graphdiyne-promoted highly efficient photocatalytic activity of graphdiyne/silver phosphate pickering emulsion under visible-light irradiation. *ACS Applied Materials and Interfaces*, vol. 11, no. 3, pp. 2684-2691, 2019.

[23] D. J. Martin, G. Liu, S. J. A. Moniz, Y. Bi, A. Beale, J. Ye, and H. Tang, "Efficient visible driven photocatalyst, silver phosphate: Performance, understanding and perspective," *Chemical Society Reviews,* vol. 44, no. 21, pp. 7808-7828, 2015.

[24] F. Dong, H. Liu, W. K. Ho, M. Fu, and Z. Wu, "$(NH_4)_2CO_3$ mediated hydrothermal synthesis of N-doped $(BiO)_2CO_3$ hollow nanoplates microspheres as high-performance and durable visible light photocatalyst for air cleaning," *Chemical Engineering Journal,* vol. 214, pp. 198-207, 2013.

[25] Y. Mao, T. J. Park, F. Zhang, H. Zhou, and S. S. Wong, "Environmentally friendly methodologies of nanostructure synthesis," *Small.*, vol. 3, no. 7, pp. 1122-1139, 2007.

[26] I. S. Neira, Y. V. Kolen'ko, O. I. Lebedev, G. V. Tendeloo, H. S. Gupta, F. Guitian, and M. Yoshimura, "An effective morphology control of hydroxyapatite crystals via hydrothermal synthesis," *Crystal Growth and Design*, vol. 9, no. 1, pp. 466-474, 2009.

[27] A. Amirulsyafiee, M. M. Khan, and M. H. Harunsani, "Ag_3PO_4 and Ag_3PO_4–based visible light active photocatalysts: Recent progress, synthesis, and photocatalytic applications," *Catalysis Communications*, vol. 172, p. 106556, 2022.

[28] H. N. Ng, C. Calvo, and R. Faggiani, "A new investigation of the structure of silver orthophosphate," *Acta* Crystallographica, vol. B34, pp. 898-899, 1978.

[29] S. H. Sohrabnezhad, "Study of catalytic reduction and photo-degradation of methylene blue by heterogeneous catalyst," *Spectrochimica Acta Part A: Molecular and Biomolecular Spectroscopy,* vol. 81, no. 1, pp. 228-235, 2011.